



Restoration of the Patient-Specific Anatomy of the Proximal and Distal Parts of the Humerus: Statistical Shape Modeling Versus Contralateral Registration Method

Vlachopoulos, Lazaros ; Lüthi, Marcel ; Carrillo, Fabio ; Gerber, Christian ; Székely, Gábor ; FÜRNSTAHL, Philipp

Abstract: **BACKGROUND** In computer-assisted reconstructive surgeries, the contralateral anatomy is established as the best available reconstruction template. However, existing intra-individual bilateral differences or a pathological, contralateral humerus may limit the applicability of the method. The aim of the study was to evaluate whether a statistical shape model (SSM) has the potential to predict accurately the pretraumatic anatomy of the humerus from the posttraumatic condition. **METHODS** Three-dimensional (3D) triangular surface models were extracted from the computed tomographic data of 100 paired cadaveric humeri without a pathological condition. An SSM was constructed, encoding the characteristic shape variations among the individuals. To predict the patient-specific anatomy of the proximal (or distal) part of the humerus with the SSM, we generated segments of the humerus of predefined length excluding the part to predict. The proximal and distal humeral prediction (p-HP and d-HP) errors, defined as the deviation of the predicted (bone) model from the original (bone) model, were evaluated. For comparison with the state-of-the-art technique, i.e., the contralateral registration method, we used the same segments of the humerus to evaluate whether the SSM or the contralateral anatomy yields a more accurate reconstruction template. **RESULTS** The p-HP error (mean and standard deviation, $3.8^\circ \pm 1.9^\circ$) using 85% of the distal end of the humerus to predict the proximal humeral anatomy was significantly smaller ($p = 0.001$) compared with the contralateral registration method. The difference between the d-HP error (mean, $5.5^\circ \pm 2.9^\circ$), using 85% of the proximal part of the humerus to predict the distal humeral anatomy, and the contralateral registration method was not significant ($p = 0.61$). The restoration of the humeral length was not significantly different between the SSM and the contralateral registration method. **CONCLUSIONS** SSMs accurately predict the patient-specific anatomy of the proximal and distal aspects of the humerus. The prediction errors of the SSM depend on the size of the healthy part of the humerus. **CLINICAL RELEVANCE** The prediction of the patient-specific anatomy of the humerus is of fundamental importance for computer-assisted reconstructive surgeries.

DOI: <https://doi.org/10.2106/JBJS.17.00829>

Posted at the Zurich Open Repository and Archive, University of Zurich

ZORA URL: <https://doi.org/10.5167/uzh-151091>

Journal Article

Published Version

Originally published at:

Vlachopoulos, Lazaros; Lüthi, Marcel; Carrillo, Fabio; Gerber, Christian; Székely, Gábor; FÜRNSTAHL, Philipp (2018). Restoration of the Patient-Specific Anatomy of the Proximal and Distal Parts of the

Humerus: Statistical Shape Modeling Versus Contralateral Registration Method. Journal Bone Joint Surgery America, 100(8):e50.
DOI: <https://doi.org/10.2106/JBJS.17.00829>

Restoration of the Patient-Specific Anatomy of the Proximal and Distal Parts of the Humerus

Statistical Shape Modeling Versus Contralateral Registration Method

Lazaros Vlachopoulos, MD, PhD, Marcel Lüthi, PhD, Fabio Carrillo, MSc, Christian Gerber, MD, FRCSEd(Hon), Gábor Székely, PhD, and Philipp Färnstahl, PhD

Investigation performed at Balgrist University Hospital, Zurich, Switzerland

Background: In computer-assisted reconstructive surgeries, the contralateral anatomy is established as the best available reconstruction template. However, existing intra-individual bilateral differences or a pathological, contralateral humerus may limit the applicability of the method. The aim of the study was to evaluate whether a statistical shape model (SSM) has the potential to predict accurately the pretraumatic anatomy of the humerus from the post-traumatic condition.

Methods: Three-dimensional (3D) triangular surface models were extracted from the computed tomographic data of 100 paired cadaveric humeri without a pathological condition. An SSM was constructed, encoding the characteristic shape variations among the individuals. To predict the patient-specific anatomy of the proximal (or distal) part of the humerus with the SSM, we generated segments of the humerus of predefined length excluding the part to predict. The proximal and distal humeral prediction (p-HP and d-HP) errors, defined as the deviation of the predicted (bone) model from the original (bone) model, were evaluated. For comparison with the state-of-the-art technique, i.e., the contralateral registration method, we used the same segments of the humerus to evaluate whether the SSM or the contralateral anatomy yields a more accurate reconstruction template.

Results: The p-HP error (mean and standard deviation, $3.8^\circ \pm 1.9^\circ$) using 85% of the distal end of the humerus to predict the proximal humeral anatomy was significantly smaller ($p = 0.001$) compared with the contralateral registration method. The difference between the d-HP error (mean, $5.5^\circ \pm 2.9^\circ$), using 85% of the proximal part of the humerus to predict the distal humeral anatomy, and the contralateral registration method was not significant ($p = 0.61$). The restoration of the humeral length was not significantly different between the SSM and the contralateral registration method.

Conclusions: SSMs accurately predict the patient-specific anatomy of the proximal and distal aspects of the humerus. The prediction errors of the SSM depend on the size of the healthy part of the humerus.

Clinical Relevance: The prediction of the patient-specific anatomy of the humerus is of fundamental importance for computer-assisted reconstructive surgeries.

Restoration of the normal humeral anatomy is one of the ultimate goals in reconstructive surgeries of the proximal and distal aspects of the humerus¹⁻⁷. Computer-assisted methods become increasingly important as they support the surgeons in achieving this goal.

Three-dimensional (3D) preoperative planning and intra-operative navigation techniques have been proposed for shoulder and elbow replacement surgeries^{3,8-12}, for proximal humeral fractures¹³⁻¹⁵, as well as for corrective osteotomies of the proximal and distal aspects of the humerus^{4,7,16}. This planning

Disclosure: This work was funded, in part, by the Swiss Canton of Zurich through a Highly Specialized Medicine (HSM2) grant. Additional funding was provided by the Balgrist Foundation and by the Promedica Foundation Switzerland. One author (P.F.) is a shareholder of Balgrist CARD (Computer Assisted Research and Development), which develops preoperative planning software. The **Disclosure of Potential Conflicts of Interest** forms are provided with the online version of the article (<http://links.lww.com/JBJS/E668>).

and navigation is made more difficult if the proximal or distal humeral anatomy is altered because of a fracture, malunion, or osteoarthritis. In such cases, the most critical step for achieving the ultimate goal of restoring normal humeral anatomy is the accurate preoperative assessment of the deformity⁷. The current state-of-the-art of 3D deformity assessment relies on comparison of the pathological bone model with a reconstruction template representing the normal anatomy. Typically, the mirrored contralateral model is selected as the most appropriate 3D reconstruction template^{4,6,7,13,16}. For the assessment of the deformity, 3D surface models of the pathological humerus and the contralateral (healthy) humerus are generated with the use of computed tomography (CT) scans of both sides. A surface registration method is applied to superimpose the pathological model on the reconstruction template and to quantify the deformity. However, most methods presented to date^{4,6,7,16} rely on a healthy contralateral anatomy and, therefore, the applicability of the 3D computer-assisted planning is limited if both sides have a pathological condition.

Another approach would be to use a statistical shape model (SSM), a computer-generated model encoding the variation

within the population, to predict the pretraumatic anatomy of the humerus from the healthy parts of the posttraumatic bone models. In a clinical setting, for example, the proximal part of the humerus might be pathological (i.e., fractured or mal-united). The humeral segment distal to the pathological area can be used to predict the proximal anatomy. The size of the distal humeral segment is thereby determined according to the extent of the pathological region.

The aims of the present study were to evaluate the accuracy of the prediction of an SSM and to analyze the influence of the size of the healthy part of the humerus on the prediction of the proximal or distal humeral anatomy. For comparison with the state-of-the-art method, we evaluated, using the same segments of the humerus, whether the SSM or the contralateral anatomy yielded a more accurate reconstruction template.

Materials and Methods

Three-dimensional triangular surface models of 100 paired humeri (50 right and 50 left) without a pathological condition were created from the data from full-body CT scans

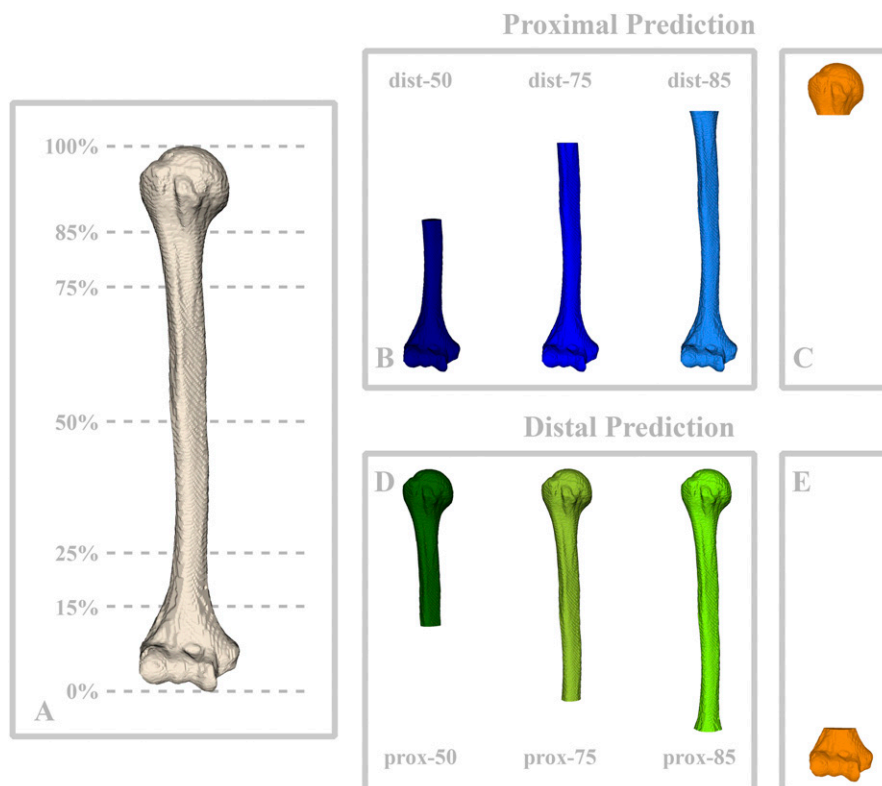


Fig. 1
Figs. 1-A through 1-E Definition of the segments. **Fig. 1-A** The right-side humeral models were subdivided into segment models of different lengths. **Fig. 1-B** For the prediction of the proximal part of the humerus (proximal prediction), we created segments of the distal humerus of predefined length: 50%, 75%, or 85% of the humerus (blue segments). **Fig. 1-C** The head segment (orange) was used to quantify the proximal humeral prediction (p-HP) errors. **Fig. 1-D** For the prediction of the distal part of the humerus (distal prediction), we created segments of the proximal part of the humerus of predefined length: 50%, 75%, or 85% of the humerus (green segments). **Fig. 1-E** The elbow segment (orange) was used to quantify the distal humeral prediction (d-HP) errors.

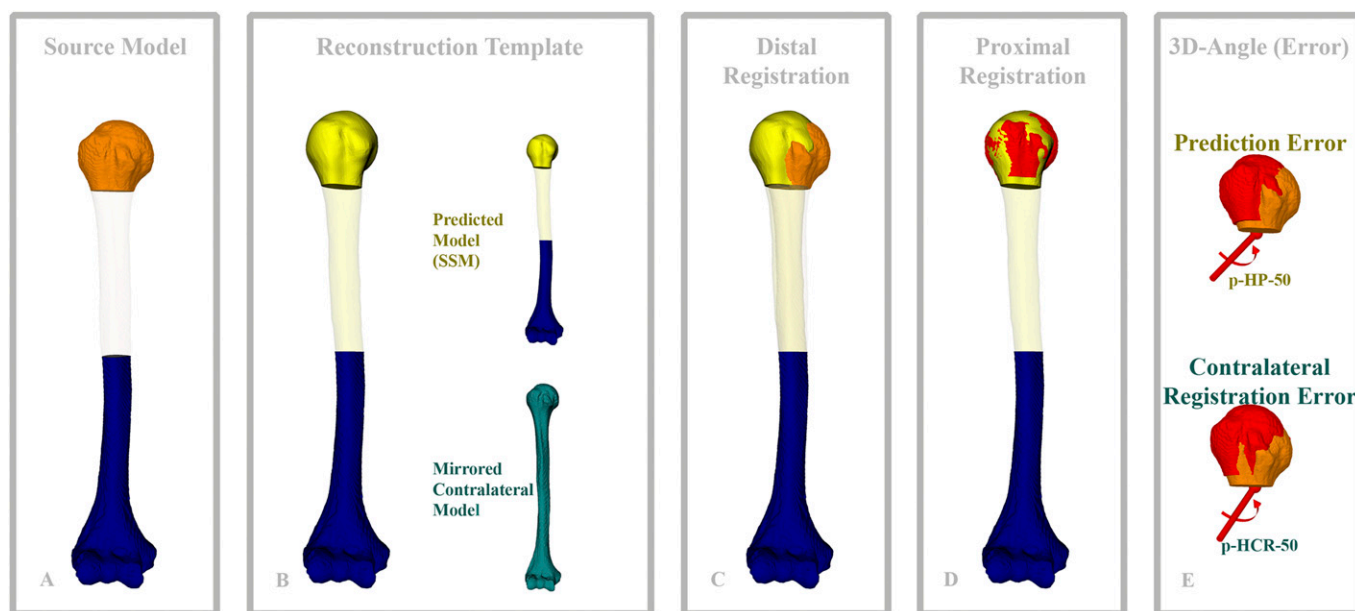


Fig. 2

Figs. 2-A through 2-E Evaluation of the humeral prediction error of the SSM and the contralateral registration error of the CRM. **Fig. 2-A** Illustration of the original bone model with the distal-50% segment (blue) used to predict the proximal humeral anatomy or for the registration with the mirrored contralateral model. The head segment (orange) is used to quantify the prediction error or the contralateral registration error. **Fig. 2-B** The predicted model (SSM) or the mirrored contralateral model (CRM) is used as a reconstruction template. **Fig. 2-C** After registration of the distal segment (blue segment) of the original bone models and the reconstruction template, the difference between the original bone model (orange) and the prediction (yellow) becomes obvious. **Fig. 2-D** The ICP algorithm was used to superimpose the head segment (red) of the original bone model on the predicted bone model. **Fig. 2-E** The 3D rotation of the head segment between the distal registration (orange) and the proximal registration (red) was expressed in axis-angle representation. This corresponds to the prediction error if the predicted model was used as a reconstruction template and to the contralateral registration error if the mirrored contralateral model was used as a reconstruction template.

of 50 cadaveric specimens. The CT data were provided by the Swiss Institute for Computer Assisted Surgery (SICAS) and were acquired using either a Siemens Somatom Emotion 6 or a Siemens Somatom Definition Flash CT scanner. The in-plane (xy) resolution of the CT scans ranged between 0.9×0.9 mm and 1.27×1.27 mm. The slice thickness varied from 0.5 to 0.6 mm. The average age of the individual donors was 52.1 ± 20.0 years (median, 52 years; range, 19 to 90 years). There were 32 male and 18 female cadavers. The average height (and standard deviation) was 172.4 ± 8.7 cm (median, 171 cm; range, 154 to 187 cm), and the average weight was 68.4 ± 16.9 kg (median, 68 kg; range, 37 to 108 kg). Segmentation of the humeri was performed in an automatic fashion using a previously described segmentation algorithm¹⁷. Three-dimensional triangular surface models were created using the marching cubes algorithm¹⁸. The models were also used in previous studies^{6,19}.

Generation of the SSM

For the SSM, we used the models of the 50 right humeri. The 3D triangular meshes were brought into correspondence using a nonrigid registration algorithm²⁰. Subsequently, all meshes were rigidly aligned using Procrustes alignment²¹ to 1 humeral model. An SSM of the aligned meshes was built by

performing a principal component analysis²². Hence, the resulting SSM encoded the mean shape of the humeri as well as the variation within the study population, which is represented by the principal components. The SSM was created using the open source software Scalismo (University of Basel), which was developed and has been maintained by one of the authors of the present study. The mathematical details of the statistical shape modeling have been described previously²³.

Evaluation Method for the SSM

Leave-one-out cross-validation was performed to evaluate the accuracy of the prediction. We defined the term *proximal prediction* as the use of prior knowledge of a distal humeral segment to predict the proximal humeral anatomy. In a similar manner, we defined the term *distal prediction*. To predict an assumed pathological part of a selected humerus, an SSM was calculated from all remaining humeri (49 humeri) except the selected one. The experiments were repeated for all 50 right humeri. To simulate the clinical situations and particularly to evaluate the effect of the size of the segments on the prediction error, we created segments of predefined length (prior knowledge) excluding the part to predict in a standardized fashion (Fig. 1). Subsequently, the shape variation of the SSM,

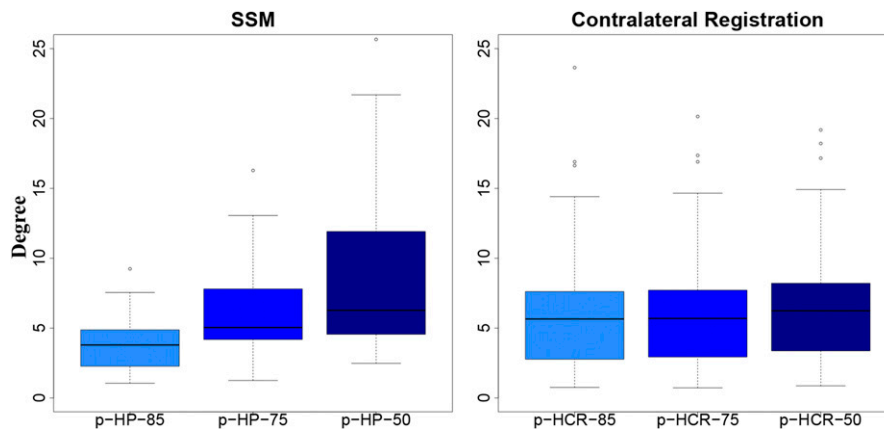


Fig. 3
Proximal humeral prediction (p-HP) errors and proximal humeral contralateral registration (p-HCR) errors. Boxplots illustrate the p-HP errors and the p-HCR errors based on the segments of the distal part of the humerus that were used for the prediction of the SSM or for the CRM. The ends of the whiskers indicate 1.5 times the IQR between the lower and upper quartile, and outliers are denoted with a circle.

which was the best fit for these segments, was determined and used as a predictor for the remaining humerus. For the proximal predictions, we defined the distal 50%, 75%, or 85% of the humerus as prior knowledge (Fig. 1). For the distal predictions, we defined the proximal 50%, 75%, or 85% of the humerus as prior knowledge (Fig. 1). We analyzed the humeral prediction (HP) error, which is defined as the deviation of the predicted (bone) model from the original (bone) model (Figs. 1-C and 1-E).

In total, we performed 6 predictions for each humerus. We calculated the errors for the 3 proximal humeral predictions (p-HPs): p-HP-50, p-HP-75, and p-HP-85, with the distal 50% (dist-50), dist-75, and dist-85 segments used as prior knowledge (Fig. 1-B). Likewise, we calculated the errors for the 3 distal humeral predictions (d-HPs): d-HP-50, d-HP-75, and d-HP-85, with the proximal 50% (prox-50), prox-75, and prox-85 segments used as prior knowledge (Fig. 1-D).

We calculated 50 SSMs with 49 models each. With these SSMs, we performed 6 predictions (with 3 proximal and 3 distal segments), resulting in 300 predictions in total.

Quantification of the Prediction Errors

The aim of reconstructive surgery, i.e., the use of corrective osteotomy or shoulder replacement surgery in the case of an altered proximal humeral anatomy, is to restore the orientation of the humeral head and of the humeral length. Any deviation of the predicted model from the original model results in an error in the restoration of the humeral anatomy. For the quantification of the errors, we used a method similar to the current state-of-the-art technique of 3D preoperative deformity assessment in corrective osteotomies of the humerus^{4,6,7,16}, hereafter termed the *contralateral registration method* (CRM). The main difference is that, in the CRM, the mirrored contralateral (bone) model is the reconstruction template, while in the SSM method, the predicted model is the reconstruction

TABLE I Proximal Humeral Prediction Errors and Proximal Humeral Contralateral Registration Errors for Each Selected Segment and P Values of the Post Hoc Analysis*

Segment	p-HP Error or p-HCR Error (deg)				P Value†				
	Mean	SD	Median	Range	p-HP-75	p-HP-50	p-HCR-85	p-HCR-75	p-HCR-50
p-HP-85	3.8	1.9	3.8	1.1-9.2	<0.0001	<0.0001	0.001	<0.001	<0.001
p-HP-75	6.1	3.2	5.0	1.3-16.3		<0.0001	0.80	0.79	0.40
p-HP-50	8.9	5.6	6.3	2.5-25.7			0.03	0.04	0.09
p-HCR-85	6.5	4.7	5.5	0.8-23.5				<0.0001	<0.0001
p-HCR-75	6.5	4.6	5.5	0.8-20.4					<0.0001
p-HCR-50	6.9	4.6	6.3	0.8-19.3					

*The Friedman rank-sum test revealed a significant effect of the selected segments on the p-HP and p-HCR errors (chi-square, 61.5; $p < 0.0001$). SD = standard deviation, p-HP = proximal humeral prediction, and p-HCR = proximal humeral contralateral registration. †Wilcoxon signed-rank tests were performed for post hoc analysis with Bonferroni correction ($p_{adj} = 0.05/15$, or approximately 0.0033, was significant).

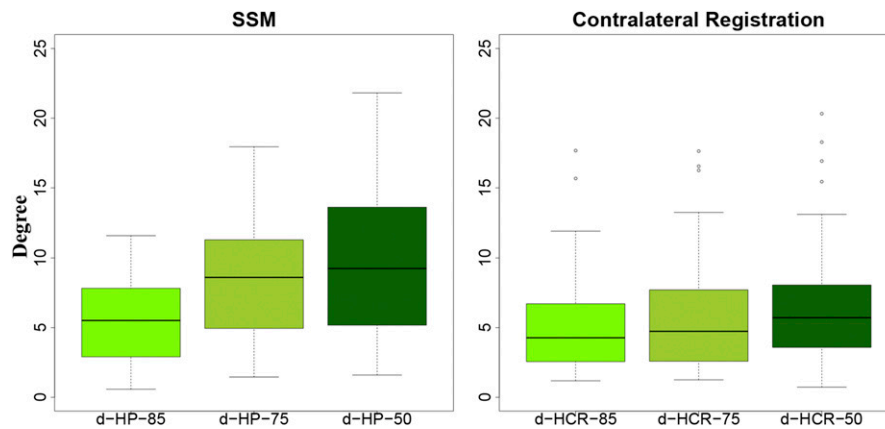


Fig. 4

Distal humeral prediction (d-HP) errors and distal humeral contralateral registration (d-HCR) errors. Boxplots illustrate the d-HP errors and the d-HCR errors based on the segments of the proximal part of the humerus that were used for the prediction of the SSM or for the CRM. The ends of the whiskers indicate 1.5 times the IQR between the lower and upper quartile, and outliers are denoted with a circle.

template. To compare the accuracy of the reconstruction templates of the SSM and the CRM in a standardized way, we used the same humeral segments for the CRM as for the SSM.

We superimposed the original model (Fig. 2-A) on the reconstruction template (Fig. 2-B), using the surface registration method termed *iterative closest point* (ICP)^{24,25}. For the p-HP error, we first performed the distal registration by aligning the distal segments of the original model and the predicted model (Fig. 2-C). Thereafter, we performed the registration of the proximal head segment onto the predicted model (Fig. 2-D). The relative 3D rotation and 3D translation of the head segment between distal (Fig. 2-C) and proximal registration (Fig. 2-D) quantifies the p-HP error. The d-HP errors were assessed accordingly for the distal prediction. The rotational components of the prediction errors were expressed in axis-angle representation (Fig. 2-E), i.e., rotation by a 3D angle about a single fixed axis²⁶. The major advantage of this representation is that it does not depend on a coordinate system. In

contrast, when using Euler angles (i.e., rotations around 3 axes of a coordinate system, representing, for example, the errors in inclination or retroversion), the rotation around 1 axis also influences the rotation around another axis. Note that the 3D angle includes errors of both inclination and retroversion and is at least as large as the smallest of these errors. The translational components of the prediction errors were expressed as the difference in humeral length between the predicted and the original model. The humeral length was expressed as the length of the longest side of the oriented bounding box of the humerus as described by Vlachopoulos et al.⁶

CRM

For the CRM, we used the mirrored contralateral models of the 50 left humeri as a reconstruction template. We analyzed the humeral contralateral registration (HCR) error, defined as the deviation of the mirrored contralateral model from the original model, in a manner similar to that for the SSM.

TABLE II Distal Humeral Prediction Errors and Distal Humeral Contralateral Registration Errors for Each Selected Segment and P Values of the Post Hoc Analysis*

Segment	d-HP Error or d-HCR Error (deg)				P Value†				
	Mean	SD	Median	Range	d-HP-75	d-HP-50	d-HCR-85	d-HCR-75	d-HCR-50
d-HP-85	5.5	2.9	5.5	1.1-11.6	<0.0001	<0.0001	0.61	0.94	0.25
d-HP-75	8.7	4.6	8.6	1.5-17.9		<0.0001	0.001	0.007	0.05
d-HP-50	9.9	5.7	9.3	1.6-21.8			<0.0001	<0.001	0.09
d-HCR-85	5.2	3.7	4.0	1.1-17.7				<0.0001	<0.0001
d-HCR-75	5.7	4.3	4.7	1.3-17.7					<0.001
d-HCR-50	6.7	4.5	5.7	0.7-20.5					

*The Friedman rank-sum test revealed a significant effect of the selected segments on the d-HP and d-HCR errors (chi-square, 52.1; $p < 0.0001$). SD = standard deviation, d-HP = distal humeral prediction, and d-HCR = distal humeral contralateral registration. †Wilcoxon signed-rank tests were performed for post hoc analysis with Bonferroni correction ($p_{adj} = 0.05/15$, or approximately 0.0033, was significant).

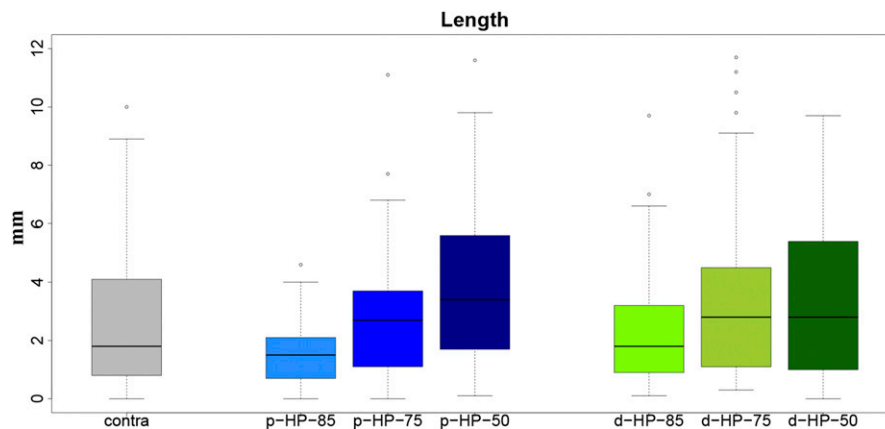


Fig. 5
Differences in humeral length. Boxplots illustrate the error in humeral length if the contralateral anatomy is used as a reconstruction template (contra) or as the difference between the predicted humeral anatomy and the original bone models. The ends of the whiskers indicate 1.5 times the IQR between the lower and upper quartile, and outliers are denoted with a circle.

In total, we yielded the 6 HCR errors per humerus, including 3 proximal HCR errors, p-HCR-50, p-HCR-75, and p-HCR-85, with the dist-50, dist-75, and dist-85 segments used for the registration; and 3 distal HCR errors, d-HCR-50, d-HCR-75, and d-HCR-85, with the prox-50, prox-75, and prox-85 segments used for the registration.

Statistical Analysis

The Mauchly sphericity test revealed a violation of the assumption of sphericity. Therefore, we applied the nonparametric Friedman rank-sum test with the segment as a group factor and the individuals as a block factor to analyze the effect of the defined segments on the HP error and the HCR error, as well as on the error in humeral length. Post hoc analysis was

performed with the Wilcoxon signed-rank test and Bonferroni adjustment. The significance level was set at $p < 0.05$. For graphical visualization, Tukey boxplots were used, with the ends of the whiskers indicating 1.5 times the interquartile range (IQR) between the lower and upper quartiles, and outliers denoted with a circle. The mean, standard deviation, median, and range of the error in humeral length as well as the rotational errors were calculated from the absolute values.

Results

Restoration of the Proximal Part of the Humerus

The p-HP-85 error was significantly smaller than any other error. The p-HP-75 error was significantly smaller ($p < 0.0001$) than the p-HP-50 error (Fig. 3, Table I).

TABLE III Comparison of Humeral Length Errors in the Contralateral Registration Modeling and Statistical Shape Modeling

Segment	Length Error* (mm)				P Value†					
	Mean	SD	Median	Range	p-HP-85	p-HP-75	p-HP-50	d-HP-85	d-HP-75	d-HP-50
Contra.	2.7	2.5	1.8	0.0-10.0	0.02	0.57	0.03	0.32	0.19	0.37
p-HP-85	1.6	1.1	1.5	0.0-4.6		0.002	<0.0001	0.02	0.002	<0.001
p-HP-75	2.8	2.2	2.7	0.0-11.1			0.003	0.25	0.19	0.53
p-HP-50	4.2	3.6	3.4	0.1-15.0				<0.001	0.20	0.24
d-HP-85	2.4	2.0	1.8	0.1-9.7					0.02	0.04
d-HP-75	3.5	3.1	2.8	0.3-11.7						0.87
d-HP-50	3.4	3.0	2.8	0.0-12.7						

*For the contralateral registration model (Contra.), the mean humeral length error represents the difference between the bilateral humeri of each individual patient. For the remaining (statistical shape) models, the mean errors represent the difference between each individual patient's humeral anatomy predicted from the entire population and of the original bone model for the same patient. All values are calculated from the absolute differences. The Friedman rank-sum test revealed a significant effect of the selected segments on the humeral length (chi-square, 19.7; $p = 0.003$). SD = standard deviation, p-HP = proximal humeral prediction, and d-HP = distal humeral prediction. †The p values are from the post hoc analysis. The Wilcoxon signed-rank test was performed for post hoc analysis with Bonferroni correction ($p_{adj} = 0.05/21$, or approximately 0.0023, was significant).

Restoration of the Distal Part of the Humerus

The d-HP errors were not significantly different from the d-HCR errors with the same segments ($p \geq 0.007$) (Fig. 4, Table II).

Restoration of the Humeral Length

The error in length did not differ significantly between use of the SSM (reflecting a prediction based on the entire population) and use of the CRM (reflecting only the same individual). (Fig. 5, Table III).

Discussion

The reliability of the reconstruction template is of fundamental importance^{7,19} since any deviation from the original model results in an error in the restoration of the humeral anatomy. The contralateral anatomy has been proposed as the best available reconstruction template^{4,7,27-29}. Furthermore, recent studies have highlighted the potential of SSMs for predicting the normal bone anatomy^{5,30}. We evaluated whether an SSM has the potential to accurately predict the pretraumatic anatomy of the proximal and distal parts of the humerus. We analyzed the accuracy of the reconstruction templates, i.e., the predicted models of the SSM and the mirrored contralateral anatomy. Note that, in the present study, we used humeral models without a pathological condition, since it is the only possible and correct way to analyze the accuracy of a new method. Therefore, in an ideal case, the reconstruction template and the original model should be identical, and the error should be zero.

We demonstrated that the prediction errors of the SSM depend on the size of the part of the bone used for the fitting of the SSM. Therefore, the whole healthy segment of the humerus should be used for the prediction of the anatomy when the method is used clinically. The HCR errors also decreased significantly with increasing size of the healthy part of the humerus. However, the size effect of the healthy part was smaller for the CRM than for the SSM.

Our study independently obtained results similar to those in the work recently reported by Poltaretskyi et al.⁵. Since the results from both studies are in agreement, these findings support the ability of SSMs to predict the pretraumatic anatomy of the humerus. The results of the proximal prediction with the dist-85 segment can be compared with the “missing epiphysis and metaphysis” results in the study by Poltaretskyi et al.⁵. However, our prediction error (mean, $3.8^\circ \pm 1.9^\circ$) includes both errors in retroversion and retrotorsion and was not larger than any of the errors of retroversion (mean, $3.8^\circ \pm 2.9^\circ$) and inclination (mean, $3.9^\circ \pm 3.4^\circ$) in the study by Poltaretskyi et al.⁵. Similarly, the error in the restoration of the humeral length was smaller with our SSM (mean, 1.6 ± 1.1 mm) compared with the previous study (mean, 2.4 ± 1.9 mm)⁵. While both studies demonstrated the value of SSMs, we also systematically analyzed the effect of the size of the segments used for the SSM and the prediction of the distal humeral anatomy and compared the results of the SSM with those of the current state-of-the-art method.

It is well accepted that initial malpositioning of a shoulder prosthesis, i.e., for proximal humeral fractures, with

excessive height and retroversion is associated with a failure involving poor functional outcome³¹. However, to our knowledge, the exact amount of clinically acceptable deviation from the normal humeral anatomy in restoration of the humeral length or angular orientation of the humeral head component is not known. Huffman et al.³² demonstrated in a biomechanical study that inferior malpositioning of ≥ 10 mm in height during hemiarthroplasty leads to significant alterations in glenohumeral joint forces, but smaller malpositioning was not investigated. The same applies for the angular orientation of articulating components, in which the maximum acceptable deviation is not yet known. Furthermore, intraoperative landmarks, i.e., the pectoralis major tendon³³, were proposed as reliable landmarks to restore the humeral length during surgery. Assuming that the distal 75% of the humerus is healthy, i.e., in the presence of a proximal humeral fracture, the mean error in restoration of the humeral length with the proposed SSM is only 2.8 mm, and the standard deviation is smaller (2.2 mm versus 5.0 mm) compared with using the pectoralis major tendon as a reference.

The accuracy with which the SSM predicted the anatomy of the distal part of the humerus was comparable with that previously reported for the CRM^{4,16}. The differences between the SSM and CRM for the reconstruction of the proximal humeral anatomy were not significant if the 50% or 75% segments were used. However, the p-HP-85 error was significantly smaller than any other error. Therefore, the SSM outperforms the CRM in selected cases. There was no significant difference in humeral length between the predicted anatomy and the contralateral anatomy. Since the contralateral anatomy is assumed to be a reliable reconstruction template for the humeral length⁶, we can conclude this also for the SSM. The main benefits of the SSM are that the acquisition of a CT scan of the contralateral anatomy is not necessary and the method is applicable even if bilateral pathological conditions are present.

One limitation of the present study is that the influence of an additional pathological condition in the assumed healthy proximal or distal segment was not analyzed and, therefore, the method might not be applicable if a combined proximal and distal posttraumatic deformity is present. On the contrary, however, Vlachopoulos et al. recently demonstrated that the CRM might still be applicable if a combined proximal and distal deformity is present, by defining segments closer to the area of interest¹⁹. Furthermore, the prediction errors of the SSM depend more on the size of the healthy part of the humerus than the CRM errors do. Although it is unlikely that $>50\%$ of the humerus is pathological and has to be predicted, the CRM in such cases might outperform the SSM. Another limitation is that no additional knowledge was included (neither for the generation of the SSM nor for the prediction). It is reasonable to assume that the prediction might improve if we incorporate more information about the patient (i.e., sex and race) as presented by Blanc et al.³⁴. The CT data were acquired with 2 different scanners and different settings. While this might be

also realistic for a clinical setting, the use of whole body scans might have negatively influenced the quality of the data and the prediction results. Furthermore, the accuracy of an SSM depends on the size of the training data. In future work, it would be interesting to evaluate the robustness of our method and the convergence in error reduction with a larger sample size. The fact that we might not yet have found the optimal method is, in our opinion, a reason for being optimistic about the SSM and would not change our conclusions in any way. In our experience, both methods (SSM and CRM) have their benefits and limitations, and therefore both approaches are not mutually exclusive or competitive but rather are complementary. Finally, it is not known how large an error in the SSM becomes of clinical importance.

In conclusion, SSMs accurately predict the patient-specific pretraumatic anatomy of the proximal and distal parts of the humerus. The prediction errors of the SSM depend on the size of the healthy part of the humerus.

Therefore, SSMs are a valuable alternative to the CRM using the mirrored contralateral anatomy as a 3D reconstruction template. These findings are particularly important when a

CT scan of the contralateral anatomy is not available or if bilateral pathological conditions are present. ■

Lazaros Vlachopoulos, MD, PhD^{1,2}
Marcel Lüthi, PhD³
Fabio Carrillo, MSc¹
Christian Gerber, MD, FRCSEd(Hon)¹
Gábor Székely, PhD²
Philipp Färnstahl, PhD¹

¹Computer Assisted Research and Development Group (L.V., F.C., and P.F.) and Department of Orthopaedics (C.G.), Balgrist University Hospital, University of Zurich, Zurich, Switzerland

²Computer Vision Laboratory, ETH Zurich, Zurich, Switzerland

³Department of Mathematics and Computer Science, University of Basel, Basel, Switzerland

E-mail address for L. Vlachopoulos: lazaros.vlachopoulos@balgrist.ch

ORCID iD for L. Vlachopoulos: [0000-0001-8526-6032](https://orcid.org/0000-0001-8526-6032)

References

- Boileau P, Walch G. The three-dimensional geometry of the proximal humerus. Implications for surgical technique and prosthetic design. *J Bone Joint Surg Br.* 1997 Sep;79(5):857-65. Epub 1997 Oct 23.
- Jeong J, Bryan J, Iannotti JP. Effect of a variable prosthetic neck-shaft angle and the surgical technique on replication of normal humeral anatomy. *J Bone Joint Surg Am.* 2009 Aug;91(8):1932-41. Epub 2009 Aug 5.
- McDonald CP, Beaton BJ, King GJ, Peters TM, Johnson JA. The effect of anatomic landmark selection of the distal humerus on registration accuracy in computer-assisted elbow surgery. *J Shoulder Elbow Surg.* 2008 Sep-Oct;17(5):833-43. Epub 2008 Jun 24.
- Murase T, Oka K, Morimoto H, Goto A, Yoshikawa H, Sugamoto K. Three-dimensional corrective osteotomy of malunited fractures of the upper extremity with use of a computer simulation system. *J Bone Joint Surg Am.* 2008 Nov;90(11):2375-89.
- Poltaretskyi S, Chaoui J, Mayya M, Hamitouche C, Bercik MJ, Boileau P, Walch G. Prediction of the pre-morbid 3D anatomy of the proximal humerus based on statistical shape modelling. *Bone Joint J.* 2017 Jul;99-B(7):927-33.
- Vlachopoulos L, Dünner C, Gass T, Graf M, Goksel O, Gerber C, Székely G, Färnstahl P. Computer algorithms for three-dimensional measurement of humeral anatomy: analysis of 140 paired humeri. *J Shoulder Elbow Surg.* 2016 Feb;25(2):e38-e48.
- Vlachopoulos L, Schweizer A, Meyer DC, Gerber C, Färnstahl P. Three-dimensional corrective osteotomies of complex malunited humeral fractures using patient-specific guides. *J Shoulder Elbow Surg.* 2016 Dec;25(12):2040-7.
- Edwards TB, Gartsman GM, O'Connor DP, Sarin VK. Safety and utility of computer-aided shoulder arthroplasty. *J Shoulder Elbow Surg.* 2008 May-Jun;17(3):503-8. Epub 2008 Feb 11.
- Gauci MO, Boileau P, Baba M, Chaoui J, Walch G. Patient-specific glenoid guides provide accuracy and reproducibility in total shoulder arthroplasty. *Bone Joint J.* 2016 Aug;98-B(8):1080-5.
- Iannotti J, Baker J, Rodríguez E, Brems J, Ricchetti E, Mesiha M, Bryan J. Three-dimensional preoperative planning software and a novel information transfer technology improve glenoid component positioning. *J Bone Joint Surg Am.* 2014 May 7;96(9):e71. Epub 2014 May 9.
- Kircher J, Wiedemann M, Magosch P, Lichtenberg S, Habermeyer P. Improved accuracy of glenoid positioning in total shoulder arthroplasty with intraoperative navigation: a prospective-randomized clinical study. *J Shoulder Elbow Surg.* 2009 Jul-Aug;18(4):515-20. Epub 2009 Jun 30.
- Tschannen M, Vlachopoulos L, Gerber C, Székely G, Färnstahl P. Regression forest-based automatic estimation of the articular margin plane for shoulder prosthesis planning. *Med Image Anal.* 2016 Jul;31:88-97. Epub 2016 Mar 3.
- Bicknell RT, DeLude JA, Kedgley AE, Ferreira LM, Dunning CE, King GJ, Faber KJ, Johnson JA, Drosdowech DS. Early experience with computer-assisted shoulder hemiarthroplasty for fractures of the proximal humerus: development of a novel technique and an in vitro comparison with traditional methods. *J Shoulder Elbow Surg.* 2007 May-Jun;16(3)(Suppl):S117-25. Epub 2007 Jan 17.
- Färnstahl P, Székely G, Gerber C, Hodler J, Snedeker JG, Harders M. Computer assisted reconstruction of complex proximal humerus fractures for preoperative planning. *Med Image Anal.* 2012 Apr;16(3):704-20. Epub 2010 Sep 29.
- Vlachopoulos L, Székely G, Gerber C, Färnstahl P. A scale-space curvature matching algorithm for the reconstruction of complex proximal humeral fractures. *Med Image Anal.* 2018 Jan;43:142-56. Epub 2017 Oct 27.
- Omori S, Murase T, Oka K, Kawanishi Y, Oura K, Tanaka H, Yoshikawa H. Postoperative accuracy analysis of three-dimensional corrective osteotomy for cubitus varus deformity with a custom-made surgical guide based on computer simulation. *J Shoulder Elbow Surg.* 2015 Feb;24(2):242-9. Epub 2014 Oct 25.
- Gass T, Székely G, Goksel O. Simultaneous segmentation and multiresolution nonrigid atlas registration. *IEEE Trans Image Process.* 2014 Jul;23(7):2931-43. Epub 2014 May 7.
- Lorensen WE, Cline HE. Marching cubes: a high resolution 3D surface construction algorithm. *ACM SIGGRAPH Computer Graphics.* 1987;21(4):163-9.
- Vlachopoulos L, Carrillo F, Gerber C, Székely G, Färnstahl P. A novel registration-based approach for 3D assessment of posttraumatic distal humeral deformities. *J Bone Joint Surg Am.* 2017 Dec 6;99(23):e127.
- Luthi M, Gerig T, Jud C, Vetter T. Gaussian process morphable models. *IEEE Trans Pattern Anal Mach Intell.* 2017 Aug 14 Aug 14. Epub 2017 Aug 14.
- Umeyama S. Least-squares estimation of transformation parameters between two point patterns. *IEEE Trans Pattern Anal Mach Intell.* 1991;13(4):376-80.
- Jolliffe IT. Principal component analysis. New York: Springer; 1986. Principal component analysis and factor analysis; p 115-28.
- Albrecht T, Lüthi M, Gerig T, Vetter T. Posterior shape models. *Med Image Anal.* 2013 Dec;17(8):959-73. Epub 2013 Jun 15.
- Besl PJ, McKay ND. A method for registration of 3-D shapes. *IEEE Trans Pattern Anal Mach Intell.* 1992 Feb;14(2):239-56.
- Chen Y, Medioni G. Object modeling by registration of multiple range images. Read at the Proceedings of the 1991 IEEE International Conference on Robotics and Automation; 1991 Apr; Sacramento, CA.
- Schneider P, Eberly DH. Geometric tools for computer graphics. San Francisco: Morgan Kaufmann; 2002.
- Eraly K, Stoffelen D, Vander Sloten J, Jonkers I, Debeer P. A patient-specific guide for optimizing custom-made glenoid implantation in cases of severe glenoid defects: an in vitro study. *J Shoulder Elbow Surg.* 2016 May;25(5):837-45. Epub 2015 Dec 15.

- 28.** McDonald CP, Peters TM, King GJ, Johnson JA. Computer assisted surgery of the distal humerus can employ contralateral images for pre-operative planning, registration, and surgical intervention. *J Shoulder Elbow Surg.* 2009 May-Jun;18(3):469-77. Epub 2009 Apr 28.
- 29.** Takeyasu Y, Oka K, Miyake J, Kataoka T, Moritomo H, Murase T. Preoperative, computer simulation-based, three-dimensional corrective osteotomy for cubitus varus deformity with use of a custom-designed surgical device. *J Bone Joint Surg Am.* 2013 Nov 20;95(22):e173. Epub 2013 Nov 22.
- 30.** Mauler F, Langguth C, Schweizer A, Vlachopoulos L, Gass T, Lüthi M, Färnstahl P. Prediction of normal bone anatomy for the planning of corrective osteotomies of malunited forearm bones using a three-dimensional statistical shape model. *J Orthop Res.* 2017 Apr 8. Epub 2017 Apr 8.
- 31.** Boileau P, Krishnan SG, Tinsi L, Walch G, Coste JS, Molé D. Tuberosity malposition and migration: reasons for poor outcomes after hemiarthroplasty for

- displaced fractures of the proximal humerus. *J Shoulder Elbow Surg.* 2002 Sep-Oct;11(5):401-12. Epub 2002 Oct 16.
- 32.** Huffman GR, Itamura JM, McGarry MH, Duong L, Gililland J, Tibone JE, Lee TQ. Neer Award 2006: biomechanical assessment of inferior tuberosity placement during hemiarthroplasty for four-part proximal humeral fractures. *J Shoulder Elbow Surg.* 2008 Mar-Apr;17(2):189-96. Epub 2008 Jan 30.
- 33.** Murachovsky J, Ikemoto RY, Nascimento LGP, Fujiki EN, Milani C, Warner JJP. Pectoralis major tendon reference (PMT): a new method for accurate restoration of humeral length with hemiarthroplasty for fracture. *J Shoulder Elbow Surg.* 2006 Nov-Dec;15(6):675-8. Epub 2006 Oct 19.
- 34.** Blanc R, Reyes M, Seiler C, Szekeely G. Conditional variability of statistical shape models based on surrogate variables. Read at the 12th International Conference on Medical Image Computing and Computer-Assisted Intervention; 2009 Sep 20-24; London, UK.